Journal of Applied Polymer Science

Shear Properties and Load–Deflection Response of Cross-Ply Glass-Epoxy Composite Short-Beams Subjected to Three-Point-Bending Tests, and the Effect of Moisture Absorption

Emilio P. Sideridis, George S. Bikakis
School of Applied Mathematical and Physical Sciences, Department of Mechanics, Strength of Materials Laboratory, National Technical University of Athens, 9 Iroon Polytechniou, Zographou, GR 157 73, Athens, Greece
Correspondence to: G. S. Bikakis (E-mail: bikakis.george@yahoo.com)

ABSTRACT: The extensive use of composites in aerospace, chemical, marine, and structural applications leads to exposure to humidity and water immersion. Hence, there is a need to study the effect of moisture absorption on the mechanical properties of composite materials, especially the matrix dominated properties, such as the interlaminar shear strength (ILSS). The horizontal shear test with a short-beam specimen in three-point-bending is used as a general method of evaluation for the shear properties in fiber-reinforced composites because of its simplicity. In this work, the ILSS of cross-ply glass-epoxy resin composites is determined in seven different fiber directions with short-beam three-point-bending tests, before and after moisture conditioning. It is found that moisture absorption reduces ILSS and stiffness of the examined composites whereas it leads to larger failure deflections. It is also found that the direction of fibers strongly affects the load–deflection response and the ILSS of the dry and conditioned specimens. © 2013 Wiley Periodicals, Inc. J. Appl. Polym. Sci. 000: 000–000, 2013

KEYWORDS: composites; degradation; mechanical properties; fibers; resins

Received 20 July 2012; accepted 20 December 2012; published online
DOI: 10.1002/app.38957

INTRODUCTION

The glass-epoxy composites are currently being used in automotive, marine, aerospace, and other lightweight structures in a variety of structural components. In many cases, composite structures must survive various environmental effects including high temperatures, humidity, and water immersion. It is therefore necessary not only to study the response and the mechanical properties of glass-epoxy composites under normal operating conditions but also to study pertinent environmental effects on their mechanical behavior.

Shear properties are very important whenever the interfacial bonding or matrix failure of a glass-epoxy composite material is critical, such as in a composite structure subjected to compression loading. Because of its simplicity, due to the reasons explained in Ref. 1, the short-beam three-point-bending test is widely used to assess the interlaminar shear strength (ILSS) of fiber-reinforced composites. It is also known that matrix dependant mechanical properties of glass-epoxy composites, including the ILSS, show significant changes due to moisture absorption.[2,3] The effect of moisture absorption on the mechanical behavior of glass-epoxy composites is often studied by submerging specimens in distilled water.[4,5]

The focus of this article is to determine the shear strength of cross-ply glass-epoxy resin composites in seven different fiber directions with short-beam three-point-bending tests, before and after moisture conditioning. Because of the importance of studying the shear properties of glass-epoxy composites with and without the presence of moisture, many researchers have carried out pertinent experimental works.[1–3,6–9] Sideridis and Papadopoulos[1] carried out three-point- bending tests of unidirectional glass-epoxy composite short-beams for different fiber directions. They determined the ILSS of these laminates in the considered fiber directions. Furthermore, the elastic constants and flexural properties were determined from bending experiments with large length/thickness ratios. Pavan et al.[2] studied the degradation of the ILSS and the compression strength of painted and unpainted glass fabric-epoxy composites that were subjected to immersion in a hot water bath. To assess the ILSS, they employed short-beams subjected to three-point bending tests. It was found that painted specimens degraded less than the unpainted ones. Srihari et al.[3] studied the degradative effects of hot artificial seawater and distilled water immersion on the ILSS and compression strength of glass fabric-epoxy composites. They also implemented experiments with short-beams under three-point-bending for the assessment of the ILSS. It was

Applied Polymer SCIENCE

concluded that both of the examined mechanical properties degraded less in the case of artificial sea water than in the case of distilled water. In the study of Roudet et al.,[7] unidirectional multilayer glass-epoxy composites were subjected to three-point-bending fatigue tests with predominant shearing. They suggested a pseudo-Wöhler curve which is in very good agreement with experimental results.

The reliability of the three-point-bending test has been demonstrated by the fact that it is being used in various experimental works.[1–3,10–14] In the work of Kam et al.,[10] the three-point-bending test has been employed for identification of elastic constants of symmetric angle-ply laminates. Based on strain measurements, they calculated the elastic constants of graphite-epoxy and glass-epoxy composites. Pauchard et al.[11] applied a stress corrosion model to the microscopic analysis of the delayed fiber failure processes occurring within water-aged unidirectional glass-epoxy composite under three-point-bending loading conditions. They found that the time dependence of the *in situ* fiber failure processes obeys a stress corrosion model.

The phenomenon of moisture absorption and its effect on the mechanical properties of glass-epoxy composites has been studied by many researchers.[4–6,15–16] Abdel-Magid et al.[4] considered unidirectional glass-epoxy composites and the combined effect due to tensile load along the fiber direction and moisture at various temperatures and durations. They recorded a positive effect of the applied stresses on this material in short term and analyzed the observed failure mechanisms at different moisture and temperature conditioning scenarios. In the work of Zheng-Liang et al.,[5] the effect of water immersion aging on the tensile strength of unidirectional angle-ply glass-epoxy composites is studied. They proposed a theoretical bridging model to predict the maximum tensile strength applicable to low moisture absorption levels. Pavan et al.[15] studied the moisture absorption characteristics of painted and unpainted glass fabric-epoxy composites that were subjected to immersion in a hot water bath. The painted specimens showed lower moisture absorption values than the unpainted ones. The adequacy of Fickian diffusion models concerning the moisture absorption was demonstrated for the examined specimens.

In this article, we present the results of an experimental study for the evaluation of the ILSS of cross-ply glass-fiber reinforced epoxy resin composites before and after moisture conditioning by submerging specimens in distilled water. To achieve this goal, short-beam laminates are prepared and tested in accordance with ASTM D2344[17] and ASTM D570[18] standards. The fiber directions change with reference to the longitudinal dimension of the beams and seven different fiber directions are considered.

It is found that moisture absorption reduces the ILSS and the stiffness of the examined composites whereas it leads to larger failure deflections. It is also found that the direction of the fibers strongly affects the load-deflection response and the ILSS of the dry and conditioned specimens. No other experimental study, concerning the ILSS measurement and load-deflection response of cross-ply glass-epoxy composites before and after moisture conditioning, using three-point-bending of short-beams with variable fiber orientations, is known to the authors.

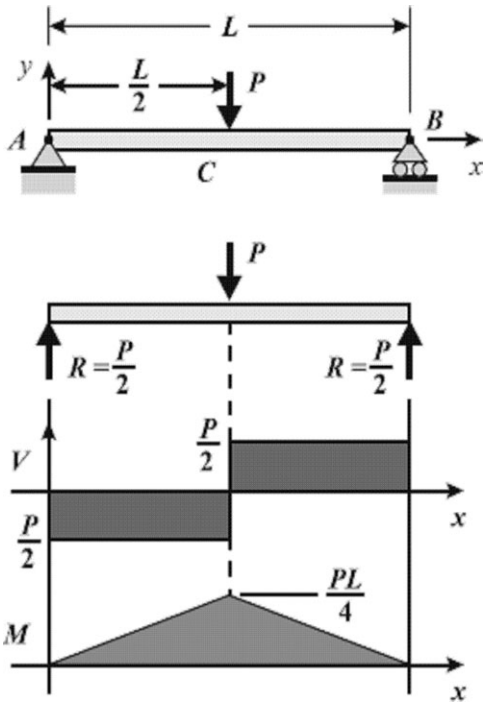

Figure 1. Three-point-bending test: geometry, shear force and bending moment diagrams.

THEORETICAL ASPECTS

In Figure 1, the geometry of the three-point-bending test is depicted along with the shear force and bending moment diagrams. The stress at any point in the beam can be calculated to a first approximation with mechanics of materials theory. The basic assumptions of this theory are summarized in Ref. 1.

The maximum bending stress is given by:

$$\sigma_x^{\max} = \frac{3PL}{2bt^2} \tag{1}$$

where P is the applied load, L is the beam's length between the supports, b and t are the dimensions of the beam cross-section.

The maximum bending stress is applied at the lower (tensile, for $y = -t/2$) and upper (compressive, for $y = t/2$) points of the beam at the center of its unsupported span ($x = L/2$). The bending stress has a linear distribution along the y-axis and becomes equal to zero for $y = 0$, along the neutral axis of the cross-section.

The maximum shear stress is given by:

$$\tau_{xy}^{\max} = \frac{3P}{4bt} \tag{2}$$

The maximum shear stress is applied at the neutral axis (for $y = 0$) of the beam at any position along its unsupported span, including the position of maximum bending stress ($x = L/2$).

The shear stress has a parabolic distribution along the y-axis and becomes equal to zero for $y = \pm t/2$, along the upper and lower points of the beam.

Taking into account eqs. (1) and (2), the two maximum stresses, simultaneously applied at the cross section of the beam at the position of the central point load ($x = L/2$), are related as follows:

$$\frac{\sigma_x^{\max}}{\tau_{xy}^{\max}} = \frac{2L}{t} \tag{3}$$

If in an experiment the shear stress at failure is τ_f and the flexure stress (tensile or compressive) at the same load is σ_f, eq. (3) can be rewritten as:

$$\frac{\sigma_f}{\tau_f} = \frac{2L}{t} \tag{4}$$

if elastic behavior is assumed.

It is seen from eq. (4) that the length to thickness ratio L/t determines the relation between the failure stresses. In this regard, this ratio can be adjusted, by changing the corresponding dimensions of the beam, to impose a shear type failure or a flexure type failure on a specimen subjected to three-point-bending test. This is reflected on the recommendations of ASTM D2344[17] standard, which is employed for the experimental part of our study.

The moisture absorption due to the submersion of the specimens in distilled water bath can be monitored by weighing the specimens periodically, starting from the moment of their initial submersion. The % moisture gain can be calculated using the following formula:[5,15,16]

$$M_t = \frac{W_t - W_0}{W_0} 100\% \tag{5}$$

where M_t is the % moisture gain at time t after the moment of initial submersion, W_t is the weight of the submerged specimen at the same time t and W_0 is the weight of the dry specimen.

The same formula is recommended in ASTM D570,[18] which is also employed for the experimental part of our study.

EXPERIMENTAL

The cross-ply glass-epoxy composite used in this study consisted of long E-glass fibers (Permaglass XE B5/1) embedded in an Araldite MY 750 HT 972 epoxy resin based on diglycidyl ether of bisphenol A together with an aromatic amine hardener. The glass fibers were contained in a volume fraction of $u_f = 0.65$. The laminates were supplied by Permali, U.K.

The volume fraction was determined, as customary, through the ignition of samples of the composite and the weighing of the residue; this gave the weight fraction of glass as $m_f = 80\%$. This result in association with the known densities of the glass and epoxy resin, gave the u_f value of 0.65.

Rectangular specimens, with a length equal to 7 cm, width b equal to 1.6 cm and mean thickness t equal to 6.5 mm were cut from laminated plates using a diamond saw cutting machine. After that, the edges of the specimens were machined with a stationary planer. By cutting the laminates along different directions, specimens with the following seven different lay-up configurations were prepared:

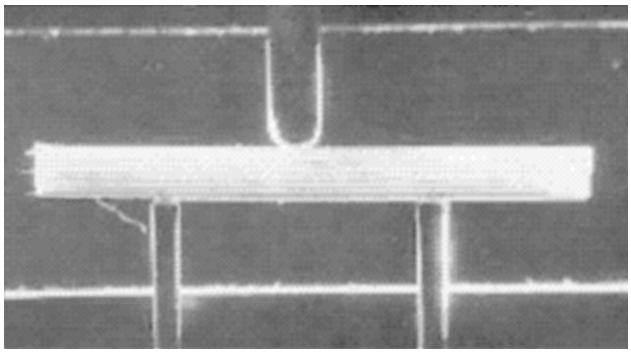

Figure 2. General arrangement of a specimen subjected to three-point-bending test.

[0°/−90°/0°/−90°/0°/−90°/0°/−90°/0°/−90°/0°/−90°/0°]
[15°/−75°/15°/−75°/15°/−75°/15°/−75°/15°/−75°/15°/−75°/15°]
[30°/−60°/30°/−60°/30°/−60°/30°/−60°/30°/−60°/30°/−60°/30°]
[45°/−45°/45°/−45°/45°/−45°/45°/−45°/45°/−45°/45°/−45°/45°]
[60°/−30°/60°/−30°/60°/−30°/60°/−30°/60°/−30°/60°/−30°/60°]
[75°/−15°/75°/−15°/75°/−15°/75°/−15°/75°/−15°/75°/−15°/75°]
[90°/0°/90°/0°/90°/0°/90°/0°/90°/0°/90°/0°/90°]

In this article, each of the above lay-up configurations will be symbolized with 0°, 15°, 30°, 45°, 60°, 75°, 90°, respectively.

The three-point-bending tests were carried out in accordance with the ASTM D2344[17] standard. The unsupported span L was set equal to 3.2 cm, to achieve an L/t ratio equal to 5, which is recommended in the ASTM D2344 standard for the determination of the ILSS of short-beams subjected to three-point-bending.

In Figure 2, the general arrangement of a simply supported composite short-beam subjected to three-point-bending is depicted. This arrangement was used for our three-point-bending experiments. The specimen is supported by two supports with rounded tips whereas the central point load is applied by an indentor, with a rounded tip as well, which is located above the specimen at the center of its unsupported span. An Instron testing machine was employed to carry out these experiments, with a maximum load capacity equal to 49,050 N. As the indentor progresses, central point load, and specimen's deflection increase. To achieve static loading conditions, the indentor moved with a slow rate of 0.2 cm/min in all cases. In each experiment, the indentor's movement started from the undeformed position and continued to move until the failure of the specimen. Figure 3 illustrates an intermediate position of the indentor, where the specimen is deformed but has not failed. The deflection at the center of the unsupported span of the specimen is equal to the grip movement of the testing machine and is obtained by the recording device of the testing machine.

Two series of three-point-bending experiments were carried out. In the first series, the specimens were dry, whereas in the second series the specimens were subjected to moisture conditioning before the bending tests. The moisture conditioning was implemented by submerging the specimens in distilled water bath maintained at 23°C, in accordance with the ASTM D570[18] standard.

Applied Polymer SCIENCE

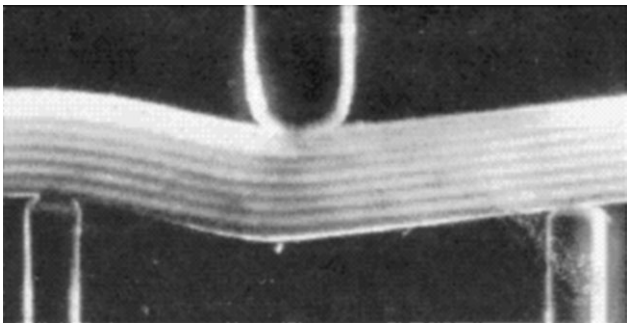

Figure 3. Deformed specimen subjected to three-point-bending test.

The procedure of moisture conditioning and moisture absorption monitoring included the following steps: The dry composite specimens were weighed and their initial weights recorded and were then immersed in the bath for a total period of eighteen days. The specimens were weighed again at four intervals of time, after 7, 10, 14, and 18 days of immersion in the bath. The moisture gain was then calculated for each time interval using eq. (5).

For each of the aforementioned lay-up configurations, four dry specimens and four conditioned specimens were subjected to three-point-bending testing.

RESULTS AND DISCUSSION

Table I contains the fiber orientation angle θ in accordance with the convention of the previous section, and the average dimensions, $t \times b$, which were calculated based on the values recorded by measuring the specimens during the three-point-bending tests. It also contains the average failure load P_f, average shear failure stress τ_f, and average flexure stress at the shear failure σ_f. For each fiber orientation angle, the average failure load value was calculated from the experimentally obtained failure loads of each dry specimen having the specific orientation angle θ. To calculate the average values of τ_f and σ_f , the shear failure stress and the corresponding flexure stress of each tested specimen were obtained using eqs. (2) and (1) respectively. Then, for each fiber orientation angle, the average τ_f and σ_f values were calculated from the corresponding previously obtained stresses at the shear failure of each dry specimen having the specific orientation angle θ. All average values of Table I are accompanied with their standard deviations. Table II contains the same quantities in Table I as determined for the conditioned specimens.

Apart from the expected experimental discrepancies, the range of failure load at each orientation angle θ, which can be observed from the corresponding standard deviations in Tables I and II, is also due to the variations of the dimensions of the specimens, especially the thickness, which plays an important role in bending.

All conditioned specimens reached saturation after immersion in distilled water bath for 10 days. This was verified by the moisture gain, calculated using eq. (5), in association with the experimental procedure described in the previous section. The moisture gain increased during the two initial time intervals and remained constant for all specimens during the following time intervals until the completion of the 18 days of immersion, yielding that the specimens were saturated with moisture. After that, the conditioned specimens were subjected to three- point-bending. Therefore, all results presented in Table II correspond to specimens saturated with moisture. In Table III, the % average moisture gain M_t of the saturated specimens is shown along with the calculated standard deviation, for each fiber orientation angle.

The values of σ_f and τ_f of Tables I and II are depicted versus θ in Figure 4, along with error bars representing their standard deviations. It can be observed from Figure 4 that under normal conditions (dry specimens), both bending and shear stresses start decreasing from 0° up to 45°, where their value is minimized, and then they start increasing up to 90°, where they almost reach the values they have for 0°. A similar behavior can be seen in Figure 4 under moisture conditions (conditioned specimens). This behavior follows the behavior of the failure load which is illustrated in Figure 5, along with error bars representing the standard deviations, as expected taking into account eqs. (1) and (2). Siderides and Papadopoulos[1] presented experimental curves of bending and shear stresses versus θ for short-beams consisting of UD glass-epoxy layers subjected to three-point-bending under normal conditions (dry specimens). In that work, the authors did not examine cross-ply laminates with variable fiber orientations, as it is done here. Furthermore, the effect of moisture absorption was not considered in Ref. 1 whereas it is considered and analyzed with a separate series of experiments in our study. In Ref. 1, both bending and shear stresses show abrupt decreases up to 45°, and then up to 90° the decreases become smooth.

The different behavior concerning the variation of bending and shear stresses versus θ, demonstrated by the experimental work

Table I. Experimental Values from Three-Point-Bending Tests of Dry Specimens

Specimens	θ (°)	t (mm)	b (cm)	P_f (N)	τ_f (Mpa)	σ_f (Mpa)
1-4	0	6.28 ± 0.14	1.63 ± 0.01	4502.79 ± 234.42	33.58 ± 1.36	348.79 ± 16.65
5-8	15	6.38 ± 0.09	1.64 ± 0.02	4734.96 ± 124.26	33.11 ± 0.41	329.41 ± 2.44
9-12	30	6.75 ± 0.10	1.60 ± 0.01	4027.01 ± 244.94	27.94 ± 1.13	264.67 ± 7.74
13-16	45	6.38 ± 0.07	1.64 ± 0.01	2893.95 ± 180.22	20.88 ± 1.55	210.20 ± 17.42
17-20	60	6.33 ± 0.09	1.63 ± 0.01	3561.03 ± 109.61	25.88 ± 0.85	262.19 ± 10.72
21-24	75	6.50 ± 0.06	1.61 ± 0.01	4024.55 ± 55.55	28.84 ± 0.28	284.07 ± 4.18
25-28	90	6.40 ± 0.07	1.60 ± 0.02	4262.45 ± 198.50	31.13 ± 0.94	311.14 ± 7.33

Table II. Experimental Values from Three-Point-Bending Tests of Conditioned Specimens

Specimens	θ (°)	t (mm)	b (cm)	P_f (N)	τ_f (Mpa)	σ_f (Mpa)
1-4	0	5.68 ± 0.14	1.65 ± 0.00	3821.68 ± 385.04	30.47 ± 2.51	343.07 ± 23.74
5-8	15	6.30 ± 0.11	1.61 ± 0.00	4295.19 ± 251.48	31.77 ± 1.87	323.16 ± 20.52
9-12	30	6.50 ± 0.27	1.61 ± 0.00	3571.70 ± 370.87	25.47 ± 1.84	250.55 ± 14.24
13-16	45	5.83 ± 0.22	1.64 ± 0.02	2308.67 ± 182.85	18.13 ± 0.95	199.20 ± 8.31
17-20	60	6.55 ± 0.12	1.62 ± 0.00	2813.88 ± 136.93	19.92 ± 0.65	194.54 ± 3.98
21-24	75	6.55 ± 0.06	1.63 ± 0.01	3552.90 ± 155.97	24.95 ± 0.73	244.32 ± 3.83
25-28	90	6.18 ± 0.11	1.58 ± 0.03	3242.25 ± 163.79	25.46 ± 0.92	268.65 ± 10.35

presented here and the experimental work presented in Ref. 1, is due to the different orientation of the fibers. In this work, taking into account the lay-up configurations of the specimens, seven of the 13 layers of the beam have their fibers initially ($\theta = 0°$) oriented along the loading direction of the beam which coincides with the longitudinal dimension L of the specimen, resulting in the maximum possible stiffness for the cross-ply lay-up and consequently the maximum failure stress. As θ increases, these fibers are gradually misaligned with reference to the loading direction of the beam, resulting in a stiffness and failure stress reduction. When θ becomes greater than 45°, in six of the 13 layers of the beam, the fibers begin to align gradually with the loading direction of the beam, resulting in a stiffness and failure stress increase. For $\theta = 90°$, the same six of the 13 layers of the beam have their fibers oriented along the loading direction of the beam, resulting in a stiffness very close to the maximum stiffness (for $\theta = 0°$) for the cross-ply lay-up and consequently, a failure stress value close to its maximum value. This is how the observed variation of the stresses depicted in Figure 4 is explained. Conversely, the orientation of the fibers in the work of Ref. 1, is initially ($\theta = 0°$) along the loading direction of the beam in all layers of the laminate, and as θ increases, all fibers are gradually misaligned with reference to the loading direction, resulting in continuous stiffness and failure stress reduction, which yield the variation of bending and shear stresses observed in Ref. 1.

It is noted that the specimens used in this study have the same length and unsupported span and almost the same thickness and width with those used in Ref. 1. Also, they consist of the same epoxy resin, glass fiber type and volume fraction of fibers. Hence, a quantitative comparison can be done between the experimental results of the two studies. By observation of the mode of failure during testing of the specimens, it was found that they have failed in interlaminar shear rather than in flexural tension or compression. This is expected since the L/t ratio is equal to five, as also described in ASTM D2344[17] standard. Figure 6 illustrates photographically the observed interlaminar shear failure mode of a tested specimen. Consequently, the experimental τ_f curves of Figure 4 are actually the ILSS curves under normal and moisture conditions. In this study, the ILSS of the dry cross-ply glass-epoxy laminates varies from 20.88 MPa (minimum) up to 33.58 MPa (maximum), depending on the orientation of the fibers. In Ref. 1, the ILSS of the unidirectional glass-epoxy laminates varies from 6.65 MPa (minimum) up to 49.06 MPa (maximum), depending again on the orientation of the fibers. These results indicate that with a unidirectional fiber reinforcement, the maximum ILSS is increased by 46% in comparison with a cross-ply fiber reinforcement whereas the minimum ILSS is decreased by 68%. These findings are expected to provide researchers and engineers, occupied with the ILSS of similar composite materials, a valuable help concerning the anticipated ILSS variations between these two fiber reinforcement configurations.

Referring to the ILSS of glass-epoxy composites, based on the qualitative and quantitative differences indicated here between cross-ply and unidirectional fiber reinforcement, useful conclusions can be drawn and used in the design of composite structures. When the ILSS is the critical design criterion, a unidirectional fiber reinforcement should be chosen rather than a

Table III. Moisture Gain Experimental Values of Conditioned Specimens

Specimens	θ (°)	M_t
1-4	0	0.11 ± 0.01
5-8	15	0.09 ± 0.00
9-12	30	0.15 ± 0.01
13-16	45	0.15 ± 0.01
17-20	60	0.12 ± 0.00
21-24	75	0.08 ± 0.00
25-28	90	0.09 ± 0.01

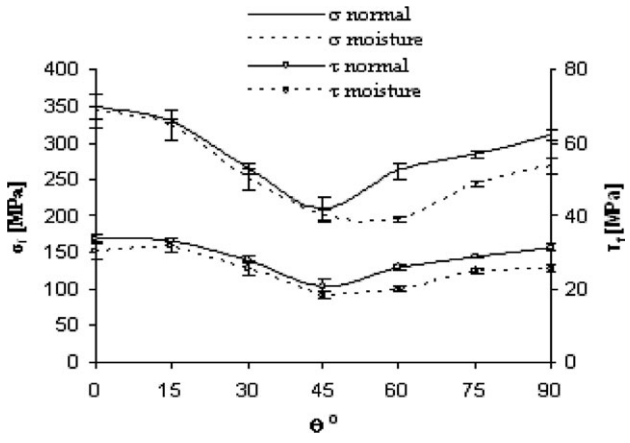

Figure 4. Variation of shear failure stresses and bending stresses versus θ for dry and conditioned specimens.

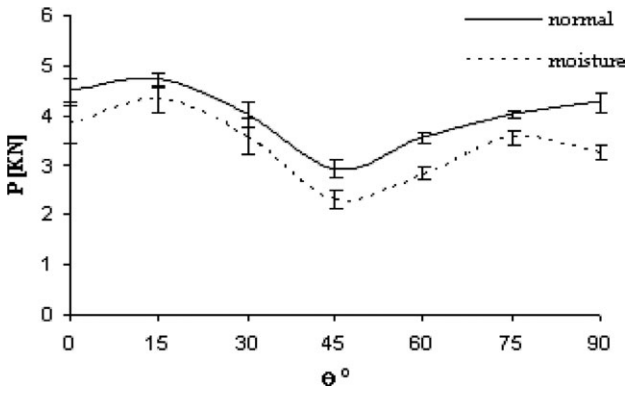

Figure 5. Variation of failure load versus θ for dry and conditioned specimens.

cross-ply reinforcement, in cases where the loading direction is known and is not expected to change with time. In such cases, the fibers should be aligned with this loading direction. Conversely, when the loading direction is unknown or variable, a cross-ply fiber reinforcement should be chosen rather than a unidirectional reinforcement. To our knowledge, these useful conclusions have not been experimentally verified elsewhere in the published literature.

As already mentioned, the variation of bending and shear stresses versus θ in Figure 4 is similar under normal and moisture conditions. It is known[4] that the glass fibers do not absorb moisture. Water that diffuses into the composite ends up either in the matrix or at the glass-epoxy interphase region. Given that during their conditioning all tested specimens reached saturation, it is expected that the matrix properties have been uniformly affected by the presence of water. Hence, the observed similarity concerning the variation of bending and shear stresses versus θ is explained by taking into account that the matrix properties have been uniformly affected by the moisture absorption and that the orientation of the fibers in dry and conditioned specimens (which governs the stress variations) is identical. This explanation is valid provided that the effectiveness of the load transfer between matrix and fiber has not been considerably affected by the presence of water at the interphase. The similarity of the variation of bending and shear stresses versus θ in Figure 4 indicates that this provision is satisfied. Furthermore, in the work of Abdel-Magid et al.,[4] who studied the combined effect due to pure tensile load along the fiber direction and moisture at various temperatures and durations on glass-epoxy composites, it is analyzed that water penetrates through the fiber-matrix interphase only at elevated temperature of 65°C, whereas this phenomenon is not taken into account at room temperature. It is reminded that in our experimental work, the specimens are conditioned at 23°C, which is practically a room temperature, a fact that, in combination with the analysis of Abdel-Magid et al., yields that in our specimens the water must have not penetrated through the fiber-matrix interphase and enhances the validity of the aforementioned provision concerning the load transfer capability between matrix and fiber. Taking into account that, Abdel-Magid et al.[4] studied unidirectional glass-epoxy composites under pure tensile loading, our findings about the fiber-matrix load transfer capability, add to the existing knowledge from the analysis of Ref. 4, since we examine different (cross-ply) composites under different (three-point-bending) loading.

In Figures 4 and 5, a comparison between dry and conditioned specimens is depicted concerning the values of τ_f , σ_f , and P_f versus θ respectively. The general trend observed in these figures is that of decreasing ILSS, bending stress at the interlaminar shear failure, and failure load, with the presence of moisture. The ILSS of the conditioned cross-ply glass-epoxy laminates varies from 18.13 MPa (minimum) up to 31.77 MPa (maximum), depending on the orientation of the fibers. Comparing these results with the corresponding values obtained for dry specimens, the maximum ILSS is decreased by 5% and the minimum ILSS is decreased by 13%, respectively, due to moisture absorption. These findings are expected to provide researchers and engineers, occupied with the effect of moisture absorption on the ILSS of similar cross-ply composites, a valuable help concerning the anticipated ILSS variations between dry composites and composites saturated with moisture at a room temperature. In Refs. 2 and 15, the ILSS reduction of glass-fabric-epoxy composites due to hygrothermal conditioning has been studied using short-beams subjected to three-point-bending tests. For a conditioning of 400 h (which is close to the 18 days of conditioning implemented in our experiments) in distilled water bath at 50°C, a 10% reduction of ILSS has been recorded whereas at the saturation level (this level has been also attained for all specimens tested in our study), which was attained in Refs. 2 and 15 at approximately 1272 h (53 days) of immersion, the ILSS reduction becomes equal to 28%. These results are comparable with the aforementioned ILSS reduction percentages recorded here, taking into account that the conditioning is not at the same temperature level (in our experiments the water bath is maintained at 23°C) and the tested materials are not identical.

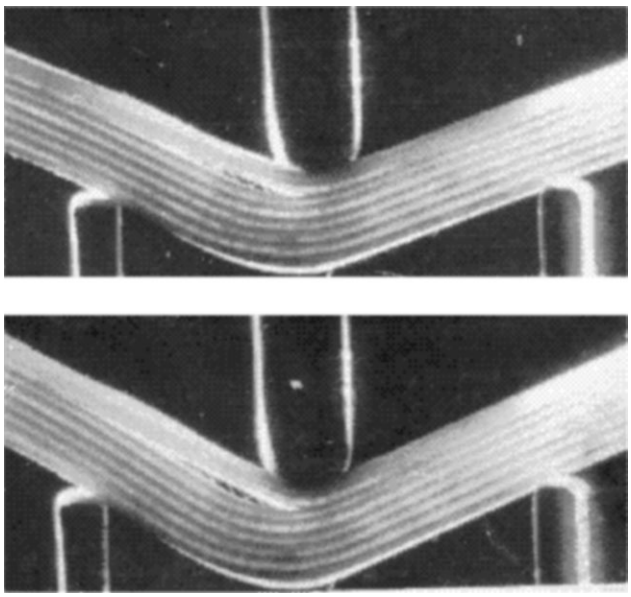

Figure 6. Observed interlaminar shear failure mode of a tested specimen.

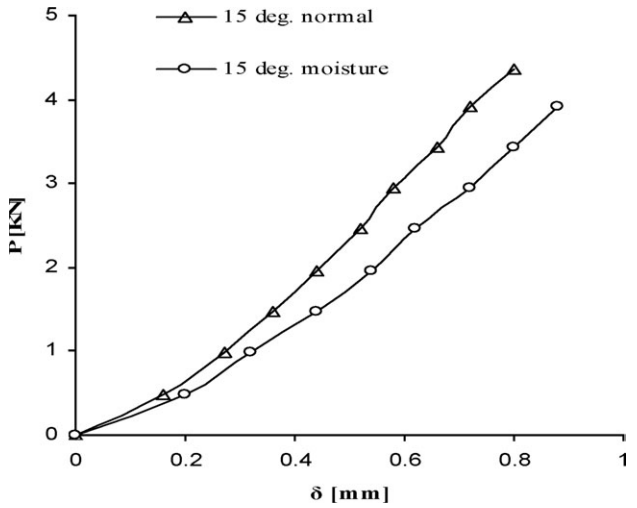

Figure 7. Load–deflection curves for $\theta = 15°$ of dry and conditioned specimens.

In Refs. 3 and 16, the ILSS reduction of glass-fabric-epoxy composites due to hygrothermal conditioning has been also studied using short-beams subjected to three-point-bending tests. For a conditioning of 400 h (which is close to the eighteen days of conditioning implemented in our experiments) in distilled water bath at 60°C, a 36% reduction of ILSS has been recorded whereas near the saturation level (this level has been also attained for all specimens tested in our study), which was attained in Refs. 3 and 16 at approximately 1152 h (48 days) of immersion, the ILSS reduction becomes more than 41%.These results indicate a more severe degradation of the ILSS in comparison with the results recorded here and in Refs. 2 and 15, due to the elevated temperature of the hot water bath.

Figure 7 illustrates a representative load-deflection diagram for the examined θ value equal to 15°, as obtained from short-beam three-point-bending experiments of dry and conditioned specimens. The trend observed in this figure is that of decreasing stiffness and failure load and that of increasing failure deflection with the presence of moisture. This is also the governing trend observed from our experimental results, obtained with a series of three-point-bending tests, for θ values other than 15°, when θ varies from 0° to 90°.

Referring to the load-deflection curves presented in the aforementioned works of Pavan et al.[2] and Srihari et al.,[3] the failure load decreases gradually as the moisture absorption increases. This trend is in agreement with our experimental results, but the failure deflection decreases in their works whereas the failure deflection increases in accordance with our experiments. We speculate that this is due to the effect of the elevated temperature of the hot water bath used in Refs. 2 and 3, which causes a more severe degradation of the ILSS, than a degradation caused in a water bath maintained at 23°C, accompanied with lower failure deflection.

The reduction of stiffness, failure load and the increase of failure deflection observed by the load–deflection diagrams is a result of the diffusion of water in the matrix. Water acts as a plasticizer and lowers the matrix modulus.[3,4,19,20] This is why the load-deflection response of the conditioned specimens indicates a reduced stiffness in comparison with the dry specimens. The failure load reduction, also illustrated in Figure 5, is associated with the previously discussed ILSS degradation due to moisture absorption and is expected taking into account eq. (2).

The phenomenon of reduced ILSS due to the presence of moisture has also been indicated in Refs 2 and 3. However, to our knowledge, the mechanism which causes this ILSS degradation has not been explained yet. This is an area for future studies in this field. Here, we note the factors that appear to influence ILSS decrease due to moisture absorption and should be taken into account in order to fully understand this phenomenon. First, the swelling strains of moisture uptake tend to relieve the internal stresses built up by the contraction due to processing thermal differences at the manufacturing stage.[4,21] This relief leads to a redistribution of the residual stress field which should be examined in association with the applied loading stresses. At the same time, the swelling strains induce stresses at the fiber/matrix interphase which may result in debonding of the fibers and/or matrix cracking. In this regard, the interphasial strength may be weakened leading to short-beam shear-strength reduction.[2–4] Consequently, the interphasial strength should also be taken into account in order to study the ILSS reduction. The matrix plasticization with the presence of water affects the polymer's mechanical properties such as stiffness, toughness and strength.[20] As the ILSS is a matrix dominated property,[1–3] the polymer matrix plasticization must also be considered as a factor influencing the ILSS degradation as well.

Referring to the increase of the failure deflection, we believe that it is caused by the matrix plasticization due to moisture absorption. The presence of a plasticizer (water) makes the matrix pliable,[4] causing the material to be more ductile and less brittle. This increase of ductility results in higher strain-to-failure values, in other words the failure of conditioned specimens is delayed in comparison with the failure of dry specimens. This

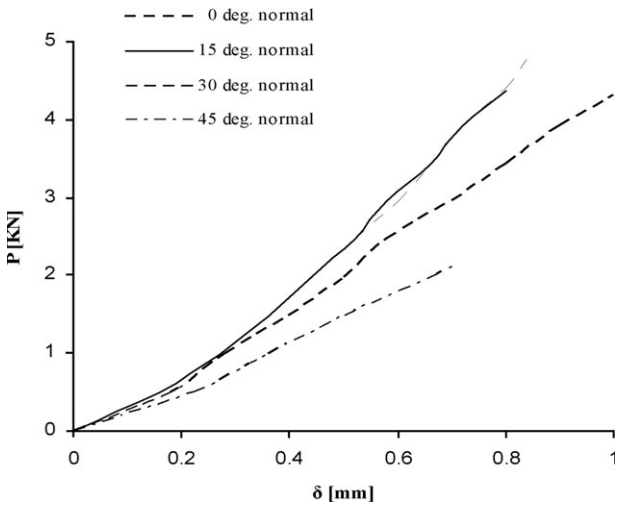

Figure 8. Load–deflection curves of dry specimens for θ values between 0° and 45°.

Applied Polymer SCIENCE

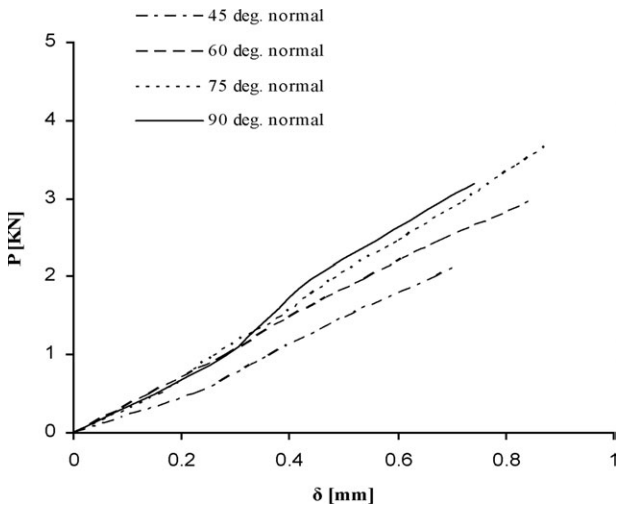

Figure 9. Load–deflection curves of dry specimens for θ values between 45° and 90°.

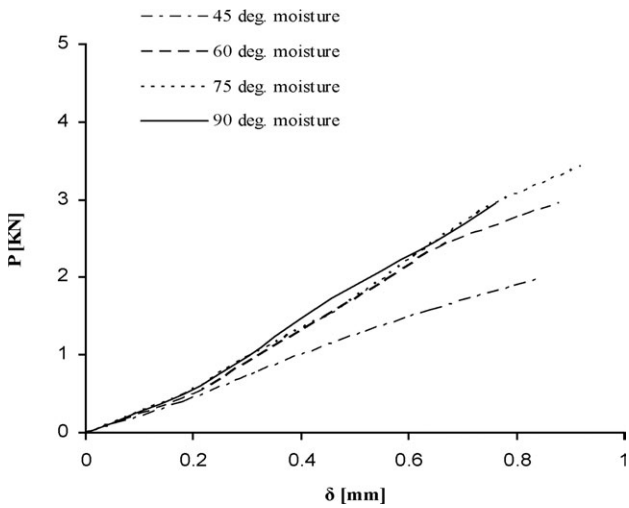

Figure 11. Load–deflection curves of conditioned specimens for θ values between 45° and 90°.

failure delay is the reason that explains the increase of the failure deflection illustrated in Figure 7. To our knowledge, this phenomenon of increased failure deflection observed in our three-point-bending tests, has not been previously studied for similar composite materials subjected to three-point-bending. It is a phenomenon that should be taken into account by researchers and engineers, when a critical design criterion of a similar composite structure is the maximum allowable deflection.

In Figures 8–11, a comparison of the load-deflection curves, as obtained from short-beam three-point-bending tests, is depicted versus θ for dry (Figures 8 and 9) and conditioned specimens (Figures 10 and 11). The governing trend demonstrated in these figures is that the slope of the curves decreases gradually when θ increases from 0° to 45° and increases gradually when θ increases from 45° to 90°. The slope, is minimized for $\theta = 45°$. In the great majority of presented curves, the observed slope and failure load variations follow the previously discussed stiffness and failure load (Figure 5) variations, which are caused by the different orientation of the fibers in the specimens.

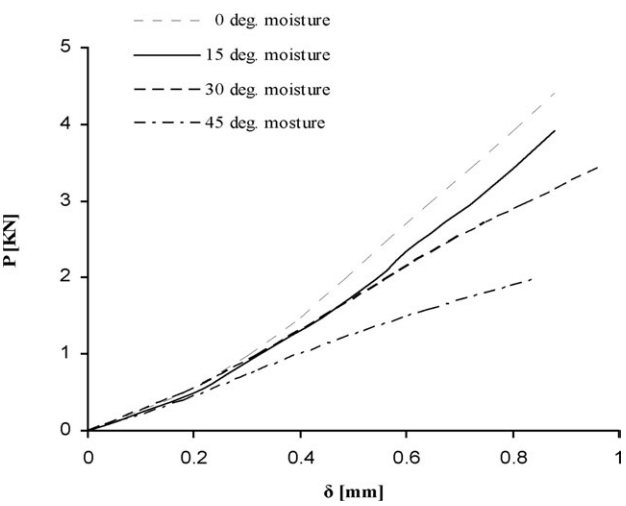

Figure 10. Load–deflection curves of conditioned specimens for θ values between 0° and 45°.

CONCLUSIONS

In this study, the ILSS of cross-ply glass-epoxy resin composites is determined in seven different fiber directions with short-beam three-point-bending tests, before and after moisture conditioning. Also, corresponding experimental load-deflection curves are presented. From the obtained results, the following conclusions are drawn:

Moisture absorption reduces the ILSS and the stiffness of the examined composites whereas it leads to larger failure deflections.

The orientation of the fibers strongly affects the ILSS and the load-deflection response of the dry and conditioned specimens.

The ILSS of the examined dry glass-fiber/epoxy-resin composite, for $u_f = 0.65$, varies from 20.88 MPa (minimum) up to 33.58 MPa (maximum), depending on the orientation of the fibers.

The ILSS varies from 18.13 MPa (minimum) up to 31.77 MPa (maximum), depending on the orientation of the fibers, when the examined composite is saturated with moisture after immersion in distilled water bath at 23°C.

For the examined composite, the similarity in the variation of shear stress and bending stress at the interlaminar shear failure versus the fiber orientation angle, observed under normal and moisture conditions, indicates that the load transfer capability between matrix and fiber is not considerably affected by short term immersion (18 days) in distilled water bath at 23°C. This finding indicates that the fiber–matrix interphase is not considerably affected by the short term immersion as well.

REFERENCES

1. Sideridis, E.; Papadopoulos, G. A. *J. Appl. Polym. Sci.* **2004**, *93*, 63.

2. Pavan, R. M. V.; Saravanan, V.; Dinesh, A. R.; Rao, Y. J.; Srihari, S.; Revathi, A. *J. Reinf. Plast. Compos.* **2001**, *20*, 1048.
3. Srihari, S.; Revathi, A.; Rao, R. M. V. G. K. *J. Reinf. Plast. Compos.* **2002**, *21*, 993.
4. Abdel-Magid, B.; Ziaee, S.; Gass, K.; Schneider, M. *Compos. Struct.* **2005**, *71*, 320.
5. Zheng-Liang, L.; Chang-Jie, L.; Kuan, H.; Tao, S. In ICCET **2010**, Proceedings of the 2nd International Conference on Computer Engineering and Technology, Chengdu, China, April 16-18, 2010; Nahadevan, V., Ed.; IEEE, **2010**.
6. Ray, B. C. *Mater. Sci. Eng. A* **2004**, *379*, 39.
7. Roudet, F.; Desplanques, Y.; Degallaix, S. *Int. J. Fatigue* **2002**, *24*, 327.
8. Li, Y.; Cordovez, M.; Karbhari, V. M. *Compos. Part B- Eng.* **2003**, *34*, 383.
9. Magalhaes, A. G.; de Moura, M. F. S. F. *NDT&E Int.* **2005**, *38*, 45.
10. Kam, T. Y.; Chen, C. M.; Yang, S. H. *Compos. Struct.* **2009**, *88*, 624.
11. Pauchard, V.; Chateauminois, A.; Grosjean, F.; Odru, P. *Int. J. Fatigue* **2002**, *24*, 447.
12. Ling, H. Y.; Lau, K. T.; Cheng, L.; Jin, W. *Smart Mater. Struct.* **2005**, *14*, 1377.
13. Yao, J.; Ziegmann, G. *Polym. Test.* **2006**, *25*, 149.
14. Pashmforoush, F.; Fotouhi, M.; Ahmadi, M. *J. Mater. Eng. Perform.* **2012**, *21*, 1380.
15. Pavan, R. M. V.; Saravanan, V.; Dinesh, A. R.; Rao, Y. J.; Srihari, S.; Revathi, A. *J. Reinf. Plast. Compos.* **2001**, *20*, 1036.
16. Srihari, S.; Revathi, A.; Rao, R. M. V. G. K. *J. Reinf. Plast. Compos.* **2002**, *21*, 983.
17. American Society for Testing and Materials (ASTM), Standard Test Method for Apparent Interlaminar Shear Strength of Parallel Fiber Composites by Short-Beam Method, ASTM D2344 Standard, **1984**.
18. American Society for Testing and Materials (ASTM), Standard Test Method for Water Absorption of Plastics, ASTM D570 Standard, **1984**.
19. Wolfrum, J.; Stang, C.; Ehrenstein, G. W. *Polym. Compos.* **2004**, *25*, 289.
20. Osswald, T. A.; Menges, G. In Materials Science of Polymers for Engineers; Hanser: New York, **1996**; Chapter 5, pp 133.
21. Nettles AT. In Basic Mechanics of Laminated composite plates; NASA Reference Publication 1351: Marshall Space Flight Center, Alabama, **1994**; Chapter VII, pp 56.